

Mechanism of Assembly of the Tyrosyl Radical–Dinuclear Iron Cluster Cofactor of Ribonucleotide Reductase

J. M. BOLLINGER, JR., D. E. EDMONDSON, B. H. HUYNH,
J. FILLEY, J. R. NORTON, J. STUBBE

Incubation of the apoB2 subunit of *Escherichia coli* ribonucleotide reductase with Fe^{2+} and O_2 produces native B2, which contains the tyrosyl radical–dinuclear iron cluster cofactor required for nucleotide reduction. The chemical mechanism of this reconstitution reaction was investigated by stopped-flow absorption spectroscopy and by rapid freeze-quench EPR (electron paramagnetic resonance) spectroscopy. Two novel intermediates have been detected in the reaction. The first exhibits a broad absorption band centered at 565 nanometers. Based on known model chemistry, this intermediate is proposed to be a μ -peroxodiferric complex. The second intermediate exhibits a broad absorption band centered at 360 nanometers and a sharp, isotropic EPR signal with $g = 2.00$.

When the reaction is carried out with $^{57}\text{Fe}^{2+}$, this EPR signal is broadened, demonstrating that the intermediate is an iron-coupled radical. Variation of the ratio of Fe^{2+} to B2 in the reaction and comparison of the rates of formation and decay of the intermediates to the rate of formation of the tyrosyl radical ($\cdot\text{Y122}$) suggest that both intermediates can generate $\cdot\text{Y122}$. This conclusion is supported by the fact that both intermediates exhibit an increased lifetime in a mutant B2 subunit (B2-Y122F) lacking the oxidizable Y122. Based on these kinetic and spectroscopic data, a mechanism for the reaction is proposed. Unlike reactions catalyzed by heme-iron peroxidases, oxygenases, and model complexes, the reconstitution reaction appears not to involve high-valent iron intermediates.

RIBONUCLEOTIDE REDUCTASES (RNR's) CATALYZE THE conversion of nucleotides to deoxynucleotides in all organisms, and hence are essential for DNA biosynthesis (1-3). *Escherichia coli* RNR, the prototype of RNR's from higher organisms, has been the subject of extensive investigation regarding its structure (2, 4) and its catalytic mechanism (1). The enzyme is composed of two subunits, B1 and B2, each of which is homodimeric (5). The large subunit, B1, binds the substrates and the allosteric effectors, and contains the cysteine residues which reduce the substrate. The small subunit, B2, contains the cofactor required for nucleotide reduction—a stable tyrosyl radical (at Y122) adjacent to an oxo-bridged dinuclear iron cluster. After the seminal experiments identifying this unusual cofactor were reported (6, 7), various physical and biochemical methods have been used in an attempt to define its detailed structure (6, 8-14). These efforts culminated with the recent report by Nordlund *et al.*, of the structure of B2, determined by x-ray crystallography (4). The structure reveals that Y122 is 5.3 Å from the nearest iron of the diferric center (Fig. 1). The proximity of the two species that had previously been inferred from physical studies (15) supports the widely held notion that the iron center generates the tyrosyl radical. The chemical mechanism of the radical generating reaction is the subject of this article.

It has become clear that the type of dinuclear non-heme iron cluster identified in B2 is a prevalent and versatile catalytic motif in nature (16). Proteins now established to contain clusters of this type include hemerythrins, which are the oxygen-carrying proteins of certain marine invertebrates (17); methane monooxygenases, the enzymes that hydroxylate methane in methanotrophic bacteria (18); and the small subunit of RNR's (5). In each of these proteins, the iron cluster functions by reaction of its different form with O₂, but the mode of reactivity is different in each class. In hemerythrins, O₂ is reversibly bound. In methane monooxygenases, O₂ is reductively

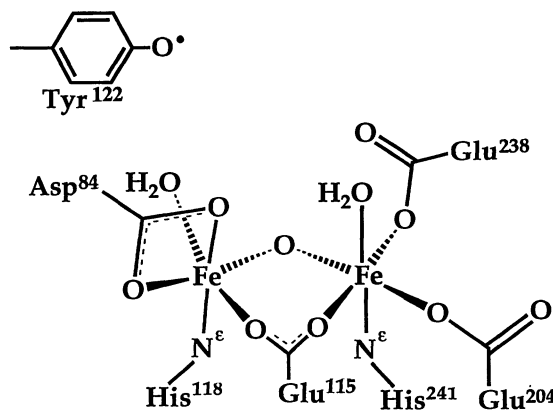


Fig. 1. Schematic representation of the dinuclear iron cluster-tyrosyl radical cofactor of native B2 (adapted from 4).

J. M. Bollinger, Jr., and J. Stubbe are in the Department of Chemistry and Biology, Massachusetts Institute of Technology, Cambridge, MA 02139. D. E. Edmondson is in the Department of Biochemistry, Emory University, Atlanta, GA 30322. B. H. Huynh is in the Department of Physics, Emory University, Atlanta, GA 30322. J. Filley and J. R. Norton are in the Department of Chemistry, Colorado State University, Fort Collins, CO 80523.

activated for two-electron oxidation of a hydrocarbon substrate. Finally, in the small subunit of RNR's, O₂ is activated for one-electron oxidation of a tyrosine residue.

A central objective in the study of these dinuclear iron proteins is to define the structural features (of the iron cluster, of the protein, or of both) that dictate the mode of reactivity toward O₂ characteristic of and unique to each protein. This objective can be achieved only with a detailed knowledge both of structure and of chemical mechanism. The former has gradually been emerging: the three-dimensional structures of two dinuclear iron cluster-containing proteins, B2 and hemerythrin (4, 17), are now known. In contrast, little information has been reported regarding the chemical mechanisms of reactions mediated by dinuclear iron clusters.

For three reasons B2 provides an unusual opportunity to study the chemical mechanism of a biologically relevant reaction mediated by a dinuclear iron cluster. First, the cloning and overproduction of the protein has allowed both purification of large quantities and preparation of site-directed mutants (19). Second, the iron center of B2 can be removed from the protein, concomitant with loss of the tyrosyl radical. Addition of Fe²⁺, in the presence of O₂, to the resulting apoprotein (apo, without the metal) leads spontaneously to reassembly of the diferric center and oxidation of Y122 (6). The ability to reconstitute B2 in this manner provides a basis for studying the tyrosine oxidation reaction. Third, the distinct spectroscopic signatures of the diferric center (ultraviolet-visible range or UV-Vis) and the tyrosyl radical (UV-Vis and EPR) allow their formation to be monitored, permitting a detailed investigation of the reaction kinetics.

We now describe such an investigation, in which stopped-flow

Fig. 2. Ultraviolet-visible absorption spectra (curve A) of the dinuclear iron cluster, and (curve B) of the tyrosyl radical. Spectrum (curve C) is the sum of (A) and (B). Spectra were recorded on a Hewlett Packard HP8452A Diode Array spectrometer. The spectrum of a sample of native B2 was acquired, then this sample was treated with hydroxyurea to reduce the tyrosyl radical (22). The spectrum of the resulting metB2 (radical-free) was subtracted from that of the native B2. The resulting difference spectrum was then divided by the tyrosyl radical concentration in the native B2 sample to give (B). The spectrum of apoB2 was subtracted from that of the metB2. This difference spectrum was then divided by the concentration of diferric cluster, which was determined by Fe analysis as [Fe³⁺]/2 (23), in the metB2 sample, to give (A). Molar absorptivities at 280 nm of $1.31 \times 10^5 \text{ M}^{-1}\text{cm}^{-1}$ for native B2 and $1.20 \times 10^5 \text{ M}^{-1}\text{cm}^{-1}$ for apoB2 were assumed (6).

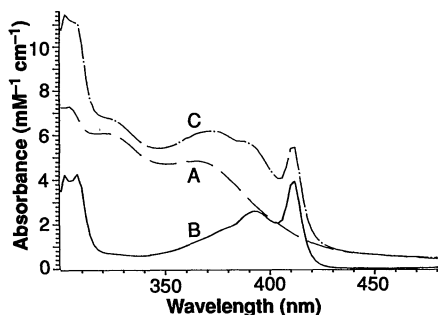
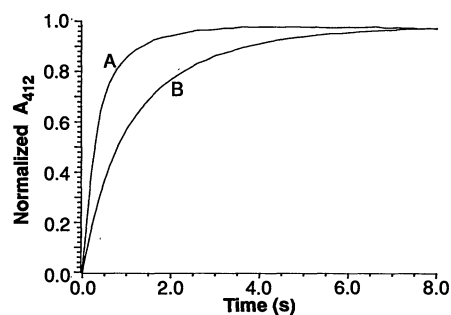
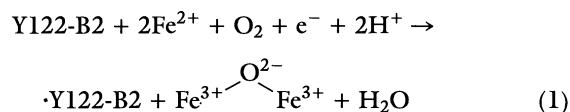


Fig. 3. Dependence of the reaction rate on the ratio Fe²⁺/B2. ApoB2 in air-saturated 100 mM Hepes buffer, pH 7.7, was mixed at 5°C with FeSO₄ dissolved in air-saturated 5 mM HNO₃. The pH after mixing was 7.6. The concentrations after mixing were (curve A) 27 μM apoB2, 59 μM Fe²⁺; (curve B) 27 μM apoB2, 250 μM Fe²⁺. The total (dead time until completion) change in A₄₁₂ for each reaction has been normalized for purposes of comparison.



absorption spectroscopy and rapid freeze-quench EPR spectroscopy have been used to identify two novel, kinetically competent intermediates in the assembly of the diferric cluster-tyrosyl radical cofactor required for nucleotide reduction. Observation of these intermediates has provided new insight into the mechanism of a biologically critical, dinuclear iron cluster-mediated oxidation reaction. This insight should aid in the more general effort to define the factors which determine the reactivity of dinuclear iron clusters.

Stoichiometry of the reaction. An essential step in the study of any reaction mechanism is determination of the stoichiometry of the reactants and the products. The available data suggest that the reaction of apoB2, Fe²⁺, and O₂ is best described as in Eq. 1. The four-electron reduction of O₂ requires



an extra electron, in addition to the three electrons resulting from production of the diferric center from two ferrous ions and the tyrosyl radical ($\cdot\text{Y122}$) from Y122. In the absence of another reductant, Fe²⁺ might be expected to provide this extra electron, in which case 3 moles of Fe²⁺ would be oxidized to produce 1 mole of $\cdot\text{Y122}$. If an alternative reductant (for example, ascorbate) were included in the reaction, the extra electron might be provided by this reductant and then only 2 moles of Fe²⁺ would be oxidized per mole of $\cdot\text{Y122}$ produced. The actual stoichiometry was determined experimentally, both in the absence and in the presence of the reductant ascorbate. In the former case 3.2 ± 0.1 moles of Fe²⁺ are required per mole of $\cdot\text{Y122}$ produced, while in the latter case (with 100 times more ascorbate than apoB2) 2.5 ± 0.1 moles of Fe²⁺ are required per mole of $\cdot\text{Y122}$ generated (20, 21). As will become apparent from the experiments described below, the discrepancy between the theoretical and experimentally determined ratios is most likely due to occasional reductive quenching, by Fe²⁺ or by ascorbate, of the tyrosyl radical-generating intermediate. Nevertheless, the determined stoichiometries corroborate the expectation that an additional electron is required to assemble the cofactor, and suggest that this electron can be supplied either by Fe²⁺ or by ascorbate.

Stop-flow absorption spectroscopy. Although the absorption spectra of the iron center and the tyrosyl radical (Fig. 2) (22) overlap, the broad bands of the iron center (curve A) at 320 nm and at 365 nm and the sharp band of the tyrosyl radical (curve B) at 412 nm allow the formation of each species to be monitored.

In order to define the time scale of the reaction, we performed a stopped-flow experiment in which 50 μM apoB2 in air-saturated 100 mM Hepes buffer, pH 7.6, was mixed at 5°C with an equal volume of 250 μM Fe²⁺ in O₂-free, 0.005 M HNO₃ (ratio of Fe²⁺ to B2, 5) (23). After being mixed, the reaction was monitored either at 412 nm or at 366 nm. Under these conditions, both A₄₁₂ and A₃₆₆ increased with apparent first-order rate constants of 1 s^{-1} ($t_{1/2} = 0.7 \text{ s}$).

With the time scale of the reaction known, the dependence of the reaction rate on Fe²⁺ concentration was investigated. The trace for 412-nm absorbance as a function of time for the reaction of apoB2 with 2.2 equivalents of Fe²⁺ (hereafter referred to as "limiting Fe²⁺") is shown in Fig. 3 (curve A) and with 10 molar equivalents of Fe²⁺ (hereafter referred to as "excess Fe²⁺") in Fig. 3, curve B. Surprisingly, nonlinear least-squares fitting of these curves gives a significantly greater apparent first-order rate constant for the limiting Fe²⁺ reaction (3 s^{-1}) than for the excess Fe²⁺ reaction (1 s^{-1}) (24).

Insight into the apparent inverse dependence of the rate constant

on $[\text{Fe}^{2+}]$ was sought by comparison of the time-dependent absorption spectra of the two reactions (Fig. 4) (25). The early spectra of both reactions suggest the occurrence of absorbing intermediates. In the "dead time" (dt, the age of the solution at the initial observation) + 0.2 s spectrum of the limiting Fe^{2+} reaction (Fig. 4A), despite the fact that only 28 percent of the final $[\cdot\text{Y122}]$ has formed (26), 70 percent of the final absorbance at 346 nm is already present. Thus, an intermediate must contribute to the absorbance in the 346-nm region of this spectrum. In the dt + 0.4 s spectrum of Fig. 4A, although 48 percent of the final concentration of $\cdot\text{Y122}$ is present, it appears that relatively little of the 320-nm and 365-nm bands of the

diferric center are present. This observation suggests that production of $\cdot\text{Y122}$ precedes formation of the diferric center under limiting Fe^{2+} conditions, which, in turn, implies that an intermediate Fe species accumulates. In the "dt + 0.2 s" spectrum of the excess Fe^{2+} reaction (Fig. 4B), although only 10 percent of the final concentration of $\cdot\text{Y122}$ has formed, 47 percent of the final absorbance at 360 nm is present. This observation might be interpreted as an indication that formation of the diferric center precedes production of $\cdot\text{Y122}$ under excess Fe^{2+} conditions. Careful examination of this spectrum, however, reveals that little of the 320-nm shoulder characteristic of the diferric center is present. In addition, the ~ 360 -nm absorbance of this spectrum occurs at slightly higher energy than the band of the diferric center. Therefore, the broad ~ 360 -nm band formed early in the excess Fe^{2+} reaction must arise from an intermediate. It thus appears that intermediates observable in the visible ultraviolet spectra are formed under both limiting Fe^{2+} and excess Fe^{2+} conditions.

In the limiting Fe^{2+} reaction, the formation of an intermediate is confirmed by the appearance of a transient absorption centered at 565 nm (Fig. 5A). The transient grows in with an apparent first-order rate constant of 8 s^{-1} , reaches maximum intensity at 0.25 s, and decays with an apparent first-order rate constant of 3 s^{-1} (27). Thus, the rate constants for formation and decay of the species giving rise to the 565-nm transient [hereafter designated (U)] imply that it is kinetically competent to be a precursor to the product, native B2. The rate constant for its decay is also the same (within experimental error) as the rate constant for the appearance of the 412-nm feature under limiting Fe^{2+} conditions (Fig. 3A) (24). This observation suggests that (U) might be directly responsible for production of $\cdot\text{Y122}$.

Interestingly, (U) is not observed in the reconstitution with excess Fe^{2+} (Fig. 5B) nor with limiting Fe^{2+} in the presence of 2.5 mM ascorbate. The failure to observe (U) in either case suggests that an excess of reductant can prevent it from accumulating to detectable amounts.

The fact that (U) forms prior to the production of $\cdot\text{Y122}$ suggests that Y122 is not involved in formation of the intermediate. A mutant B2, in which phenylalanine (F) replaces Y122, was used to test this prediction. This protein (B2-Y122F) was prepared by site-directed mutagenesis (28) in the expectation that substituting the much less easily oxidized F for Y122 would slow decomposition of the tyrosyl radical-generating intermediate, thus facilitating its detection.

The intermediate (U) is indeed observed when B2-Y122F is reconstituted with limiting Fe^{2+} (Fig. 6A). As with wild-type B2 (B2-wt), (U) is not detected in the reaction of apoB2-Y122F with excess Fe^{2+} or with limiting Fe^{2+} and ascorbate. Interestingly,

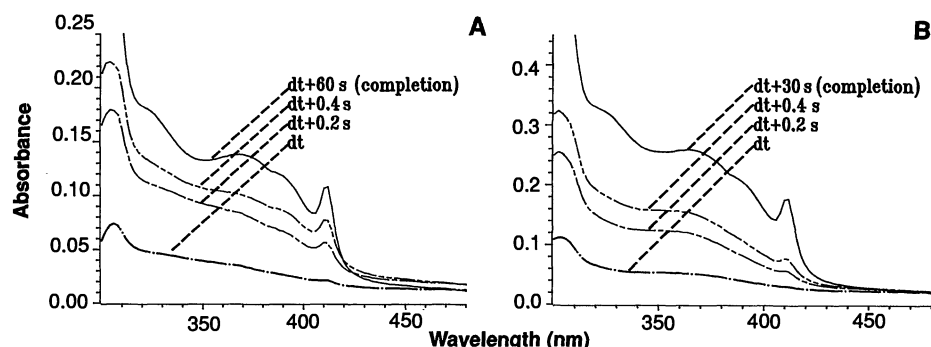


Fig. 4. Absorption spectra as a function of reaction time for reconstitution of B2: dependence on the ratio $\text{Fe}^{2+}/\text{B2}$. The reaction conditions were (A) the same as for reaction A of Fig. 3, or (B) the same as for reaction (B) of Fig. 3. The contribution to each spectrum from the protein has been subtracted away for clarity.

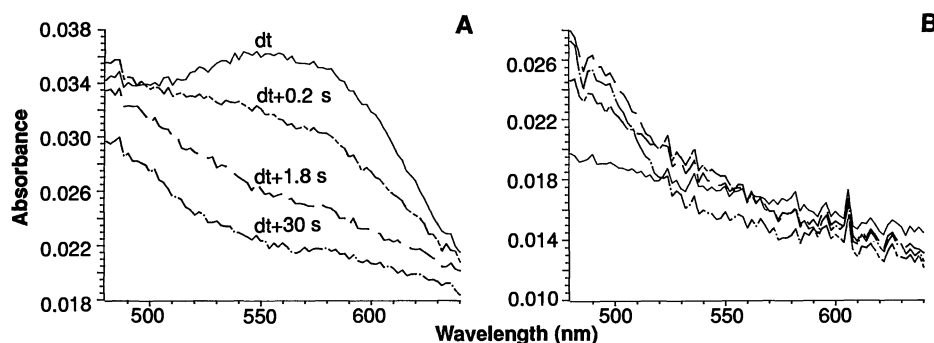


Fig. 5. Observation of the intermediate (U) in the reconstitution of B2 with limiting Fe^{2+} . The reaction conditions were (A) the same as for reaction A of Fig. 3, or (B) the same as for reaction B of Fig. 3. The time after mixing at which each spectrum was acquired is indicated in (A). The spectra in (B) were acquired at the same times as those in (A). The contribution to each spectrum from the protein has been subtracted away for clarity.

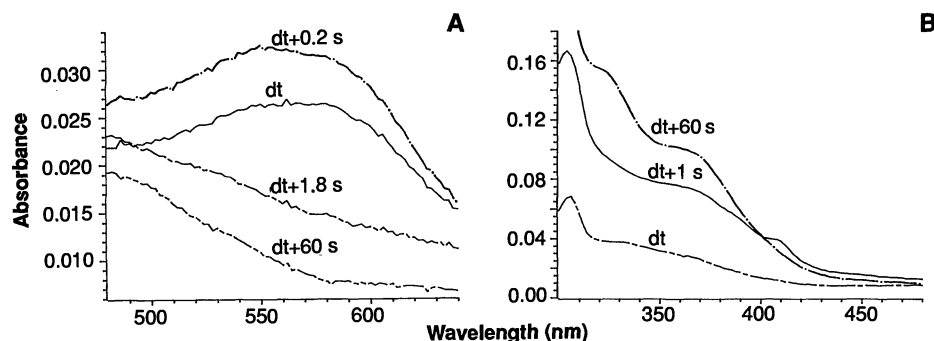


Fig. 6. Observation of (U) and a transient tyrosyl radical in the reconstitution of B2-Y122F with limiting Fe^{2+} . ApoB2-Y122F (50 μM) in air-saturated 100 mM Hepes buffer, pH 7.7, was mixed at 5°C with 110 μM FeSO_4 dissolved in air-saturated 5 mM HNO_3 . After mixing, the reaction was monitored (A) from 480 to 640 nm or (B) from 300 to 480 nm. The contribution to each spectrum from the protein has been subtracted away for clarity.

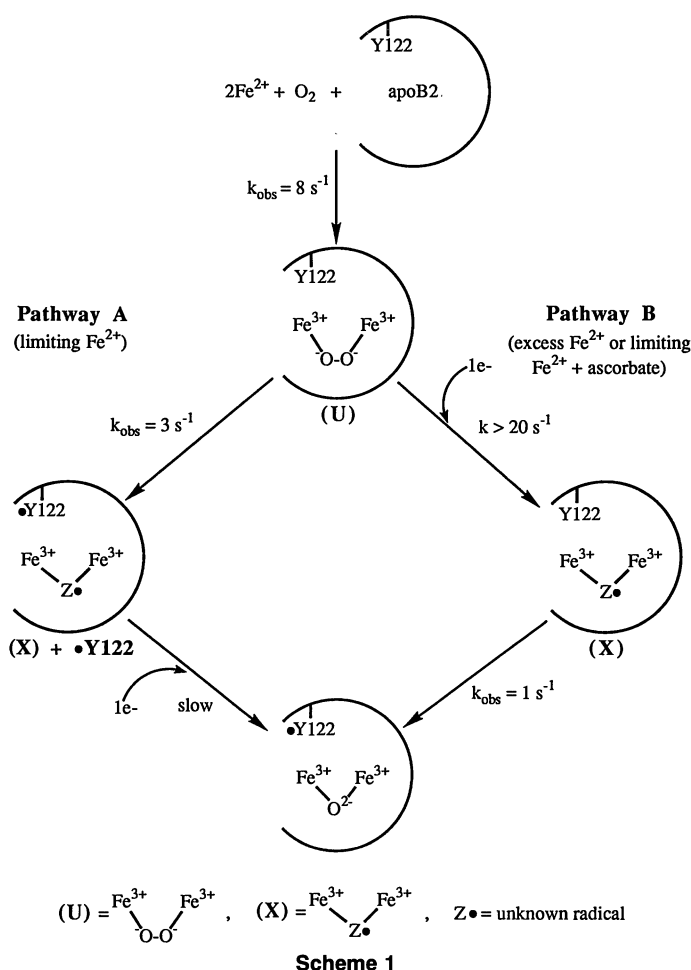
(U) decays at least twice as slowly in B2-Y122F as in B2-wt. Thus, (U) exhibits the increased lifetime in B2-Y122F expected for the tyrosyl radical-generating intermediate. Even more surprising is that a new, sharp, transient feature with a wavelength of maximum absorbance (λ_{max}) equal to 410 nm appears as (U) decays (Fig. 6B). This transient feature reaches a maximum at ~ 1 s (29) and decays with an apparent first-order rate constant of 0.07 s^{-1} . Like (U), this 410-nm transient, which strongly resembles the spectrum of a tyrosyl radical, is not observed in the reaction with excess Fe^{2+} or with limiting Fe^{2+} and ascorbate. These observations suggest that, in the absence of Y122 and under limiting Fe^{2+} conditions, an unstable radical is generated from another tyrosine in B2, concomitant with decay of (U). Taken together, the fast formation of (U); the fact that its decay is slower in B2-Y122F than in B2-wt; and the fact that, in both proteins, its decay apparently occurs as a tyrosyl radical is formed, suggest that (U) generates $\cdot\text{Y122}$ (as well as the transient tyrosyl radical seen in B2-Y122F) under limiting Fe^{2+} conditions.

A suggestion as to the structure of (U) is provided by the recent work of Menage *et al.* (30). This group synthesized the alkoxo- and carboxylato-bridged diferrous complex $\text{Fe}_2(\text{N-Et-HPTB})(\text{OBz})(\text{BF}_4)_2$ (I), in which each ferrous ion is five-coordinate. They found that exposure of (I) to O_2 at -60°C gives rise to a new species, (II), which exhibits a visible absorption spectrum ($\lambda_{\text{max}} = 588 \text{ nm}$, $\epsilon_{588} = 1500 \text{ M}^{-1} \text{ cm}^{-1}$) quite similar to the transient feature characteristic of (U) (Figs. 5A and 6) (31). In addition, they found that the analog of (II) with propionate in place of benzoate exhibits a λ_{max} nearly identical to that of (U), at 570 nm. On the basis of resonance Raman and Mössbauer spectroscopic characterization of (II), they proposed that it is the μ -(1,2) or the μ -(1,1) peroxodiferric complex resulting from addition of O_2 to (I). The expected structural analogy of (I) to the diferrous cluster of B2 [in which each ferrous ion is thought to be, at most, five-coordinate (13)] and the similarity of the absorption spectrum of (II) to that of (U), suggest that (U) is also a μ -peroxodiferric complex (32).

Proposed mechanism. The above data allow a mechanism to be proposed for the reconstitution with limiting Fe^{2+} (Scheme 1, pathway A). Addition of Fe^{2+} to apoB2 in the presence of O_2 results in rapid ($k_{\text{obs}} = 8 \text{ s}^{-1}$) formation of the μ -peroxodiferric intermediate, (U). This intermediate undergoes one-electron reduction by Y122 ($k_{\text{obs}} = 3 \text{ s}^{-1}$), simultaneously generating $\cdot\text{Y122}$ and a second intermediate, (X) [formally an Fe(IV), Fe(III) cluster]. The slow one-electron reduction of (X) by Fe^{2+} then gives the product diferric center. This mechanism is consistent with the inference made from Fig. 4A that oxidation of Y122 precedes formation of the diferric center under limiting Fe^{2+} conditions.

Pathway A of Scheme 1 does not, however, adequately account for the observations regarding the excess Fe^{2+} reaction. Specifically, the failure of (U) to accumulate despite the slower production of $\cdot\text{Y122}$ provides argument that (U) does not generate $\cdot\text{Y122}$ under excess Fe^{2+} conditions. Another pathway (Scheme 1, pathway B) is required. In this pathway, it is proposed that excess reductant rapidly ($k > 20 \text{ s}^{-1}$) (33) converts (U) to the intermediate (X), (which gives rise to 360-nm band seen in the "dt + 0.2 s" spectrum of Fig. 4B). This intermediate, still one-electron oxidized from the diferric center, then oxidizes Y122 ($k_{\text{obs}} = 1 \text{ s}^{-1}$) to generate the final products.

Since Scheme 1 proposes that (U) is rapidly reduced either by excess Fe^{2+} or by ascorbate, the mechanism is consistent with the failure of (U) to accumulate in the presence of either reductant. The proposal that two different intermediates generate $\cdot\text{Y122}$ could explain the observation that k_{obs} for growth of A_{412} is greater in the reaction with limiting Fe^{2+} than in the reaction with excess Fe^{2+} . Furthermore, this proposal has precedent in the heme-iron peroxi-



dases, in which the intermediates compound I and compound II are both competent to oxidize substrate by one electron (34, 35). Therefore, since Scheme 1 is consistent with all the stopped-flow data, it represents a reasonable working hypothesis for the mechanism of the reaction. The scheme also suggests several experiments which might be carried out to test the proposed mechanism.

Rapid freeze-quench EPR spectroscopy. The iron-containing intermediate, (X), proposed to occur in each pathway of Scheme 1 would necessarily be paramagnetic. Since it might, therefore, be EPR active, we sought evidence for (X) by using rapid freeze-quench EPR spectroscopy (36). The EPR spectrum of the reaction with limiting Fe^{2+} quenched at 0.13 s (Fig. 7A) reveals a sharp (peak-to-trough separation of 19 G at 40 K), isotropic, $g = 2.00$ singlet, quite different from the spectrum of $\cdot\text{Y122}$ (Fig. 8D). The properties of this new EPR signal are suggestive of an organic radical. Nevertheless, since the intermediate, (X), proposed in Scheme 1 is an iron species, the reaction was carried out with $^{57}\text{Fe}^{2+}$ ($I = 1/2$, where I is the nuclear spin quantum number) to test for Fe hyperfine coupling to the EPR signal. The resulting spectrum (Fig. 7B) is dramatically broadened (peak-to-trough separation of 44 G) due to the ^{57}Fe , establishing that the intermediate is an iron-coupled radical. Furthermore, since this EPR signal is also observed in the reconstitution with excess Fe^{2+} (Fig. 8A), conditions under which (U) does not accumulate, the iron-coupled radical must be distinct from (U). Therefore, it is proposed that this iron-coupled radical is the intermediate (X) of Scheme 1 (37).

The ability to trap and to detect (X) by rapid freeze-quench EPR spectroscopy provides experimental tests for several predictions made by Scheme 1. Based on the calculated rate constants of Scheme

1 and on the known $\cdot\text{Y122}/\text{B2}$ ratio after complete reconstitution (23), nearly 1 equivalent of (X) per B2 should rapidly accumulate in the reaction with excess Fe^{2+} (pathway B). Decay of (X) should occur concomitantly with formation of $\cdot\text{Y122}$. These predictions are, in fact, correct (Fig. 8). Spin quantitation of the excess Fe^{2+} reaction quenched at 0.33 s (Fig. 8A) shows that 1 ± 0.3 equivalent (38) of radical [mostly (X)] has formed in this time. The total spin concentration [(X) + $\cdot\text{Y122}$] remains unchanged (within experimental error) from 0.33 to 60 s, during which time the spectrum of (X) disappears as that of $\cdot\text{Y122}$ appears (Fig. 8, B through D).

Another prediction made by Scheme 1 is that (X) formed in pathway B (excess Fe^{2+}) might exhibit an increased lifetime in the absence of the oxidizable Y122. In fact, (X) formed in the reconstitution of B2-Y122F with excess Fe^{2+} persists longer than in B2-wt, with significant amounts (~ 0.3 equivalents) of (X) remaining after 5.6 s. The results from these EPR experiments support the mechanism proposed in pathway B of Scheme 1.

In contrast to pathway B, in which $\cdot\text{Y122}$ is produced at the expense of (X), the two species are produced in the same step of pathway A (limiting Fe^{2+}). Thus, Scheme 1 predicts that, at short times in the reconstitution with limiting Fe^{2+} , both $\cdot\text{Y122}$ and (X) should simultaneously be present in the same molecule. Dipolar interaction of the adjacent paramagnets might be expected to broaden their EPR spectra (15). To test this prediction, the EPR spectra of apoB2 mixed with limiting Fe^{2+} and quenched at times varying from 0.33 to 1.5 s were compared to the corresponding spectra of apoB2 reacted with excess Fe^{2+} . The spectra of the 0.65-s time-points are shown in Fig. 9. As predicted, the spectrum of B2 reconstituted with limiting Fe^{2+} is broader at all times from 0.33 to 1.5 s than that of B2 reconstituted with excess Fe^{2+} , and broader than that of $\cdot\text{Y122}$ alone.

Besides the postulated dipolar interaction of $\cdot\text{Y122}$ and (X), there is at least one alternative explanation for the broadening observed in Fig. 9. It is possible that, in addition to $\cdot\text{Y122}$ and (X), a third EPR active species with a broader signal at $g = 2.00$ is produced when B2 is reconstituted with limiting Fe^{2+} , but not when B2 is reconstituted with excess Fe^{2+} . An experiment with B2-Y122F argues against this possibility. If a third radical were in fact produced, it should be even more apparent in the mutant, without interference from $\cdot\text{Y122}$.

In fact, the EPR spectrum of B2-Y122F reconstituted with limiting Fe^{2+} is never broader than that of B2-Y122F reconstituted with excess Fe^{2+} . Therefore, the broadening seen in the limiting Fe^{2+} spectrum of Fig. 9 is most likely due to interaction of (X) and $\cdot\text{Y122}$. The fact that this interaction is observed in the limiting Fe^{2+} reaction (pathway A), but not in the excess Fe^{2+} reaction (pathway B), is consistent with Scheme 1.

Implications of the proposed mechanisms. In the past few years, the mechanism of assembly of the tyrosyl radical-diferrous cluster cofactor in the small subunit of RNR's has been the subject of much investigation (21, 39, 40). Proposed mechanisms have been strongly influenced by the extensive existing information regarding the mechanisms of heme-iron peroxidases (34, 35) and of heme-iron model compounds (41, 42). In most of the mechanisms advanced, the tyrosyl radical is generated by a high-valent iron-oxo intermediate [either an Fe(IV) , Fe(IV) cluster or an Fe(V) , Fe(III) cluster] which results from cleavage of the O-O bond of a peroxodiferrous intermediate (39, 40). In contrast to these proposals, a key feature of the mechanism put forth in Scheme 1 is the apparent intrinsic reactivity of the putative peroxodiferrous intermediate (U) toward one-electron reduction. In the presence of ascorbate or excess Fe^{2+} , this reduction occurs rapidly enough to prevent (U) from accumulating. When external reducing equivalents are scarce, (U) is instead reduced by Y122, but sufficiently slowly to allow its accumulation. If Y122 is mutated to a less readily oxidized residue, a more distant tyrosine (and perhaps other amino acids) can reduce (U), but more slowly still. Thus, if the assignment of (U) as a peroxodiferrous complex is correct, the data would indicate that the first intermediate competent to oxidize Y122 is not a high valent Fe species.

An issue not addressed thus far is the structure of the second reactive intermediate (X). Again on the basis of the precedent of the heme-iron peroxidases (34, 35), we thought it reasonable to propose that (X) might be a high valent iron species, possibly an Fe(IV) , Fe(III) cluster (39, 40). However, preliminary characterization of (X) by rapid freeze-quench Mössbauer spectroscopy indicates that it contains two spin-coupled, high-spin ferric ions ($S = 5/2$; S is the electron spin quantum number) (43). Since two ferric ions cannot by themselves couple to form the system spin of $1/2$ required by the $g = 2.00$ EPR signal of (X), a third constituent with half-integer

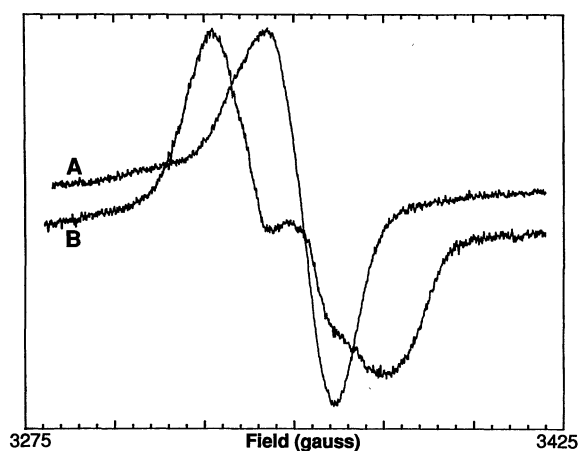


Fig. 7. Observation of the intermediate (X) by rapid freeze-quench EPR spectroscopy: demonstration of ^{57}Fe hyperfine coupling. ApoB2 (100 μM) in air-saturated 100 mM Hepes buffer, pH 7.7 was mixed at 5°C with 220 μM (curve A) $^{56}\text{Fe}^{2+}$ or (curve B) $^{57}\text{Fe}^{2+}$ in air-saturated 5 mM HCl. The reactions were quenched at 0.13 s. The spectra were recorded at 40 K on a Bruker ER 200D-SRC spectrometer equipped with an Oxford Instruments ESR 910 cryostat. The microwave power was 0.2 mW; the frequency, 9.43 GHz; the modulation frequency, 100 kHz; the modulation amplitude, 4 G; the time constant, 200 ms; and the scan time 200 s.

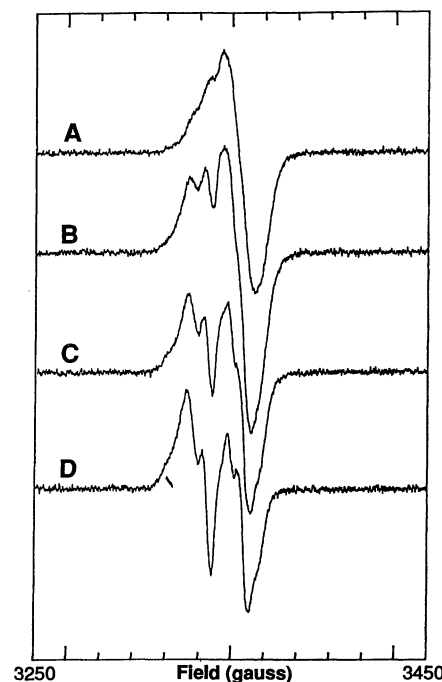


Fig. 8. Time-course of the excess Fe^{2+} reaction by rapid freeze-quench EPR spectroscopy. ApoB2 (100 μM) in air-saturated 100 mM Hepes buffer, pH 7.7 was mixed at 5°C with 1.0 mM FeSO_4 dissolved in 5 mM HNO_3 . The reactions were quenched (A) at 0.33 s, (B) at 0.65 s, (C) at 1.45 s, and (D) at 60 s. The spectra were recorded at 20 K on the spectrometer described in Fig. 7. The microwave power was 6.7 μW ; the frequency, 9.43 GHz; the modulation frequency, 100 kHz; the modulation amplitude, 4 G; the time constant, 200 ms; and the scan time, 200 s.

spin must be coupled to the cluster. This constituent is most likely an oxygen-derived or a protein-derived free radical. Therefore, since it appears likely that neither (U) nor (X) contains high valent Fe, our data suggest that high-valent Fe species may not be involved in the reconstitution reaction, in contrast to what has been proposed based on the heme-iron precedents (39, 40).

Another important implication of the mechanism proposed in Scheme 1 is the capacity of B2 to regulate reduction of (U) and (X). The intermediate (U) is rapidly reduced ($k_{\text{obs}} > 20 \text{ s}^{-1}$) (33) either by excess Fe^{2+} or by ascorbate. Conversely, the product of this reduction, (X), which is sufficiently potent an oxidant to generate $\cdot\text{Y122}$, must, in some way be protected from external reductants. The stoichiometry of 2.5 Fe^{2+} per $\cdot\text{Y122}$ in the presence of a 100-fold excess of ascorbate implies that, although ascorbate does compete with Y122 for reduction of (X), the rate constant for reduction of (X) by Y122 ($k_{\text{obs}} = 1 \text{ s}^{-1}$) is at least four times the first-order rate constant for its reduction by this large excess of ascorbate. This protection of (X), in addition to protection of $\cdot\text{Y122}$ itself, is both necessary and sufficient to ensure production of $\cdot\text{Y122}$ in the presence of the facile one-electron donors Fe^{2+} and ascorbate.

One final aspect of our study warrants discussion. The catalytic mechanism of RNR is believed to involve free radical chemistry initiated by abstraction of the hydrogen atom from the 3' position of the nucleoside diphosphate substrate (44). Until the x-ray structure of B2 revealed that Y122 is 10 Å from the nearest surface of the subunit (4), it was thought that $\cdot\text{Y122}$ was directly responsible for this hydrogen atom abstraction. The finding that Y122 is buried has led to the proposal that the function of $\cdot\text{Y122}$ in B2 is to generate, by long-range electron transfer, a protein radical on the B1 subunit. The B1 radical would then abstract the 3' hydrogen atom (45). In light of this proposal, the transient 410-nm feature observed in the reconstitution of B2-Y122F with limiting Fe^{2+} is interesting because it suggests that a tyrosine other than Y122 can transfer an electron to the iron center. This tyrosine might be important in the first step of the catalytic mechanism—electron transfer from the B1 subunit to the cofactor in B2. A sequence comparison of the small subunit of RNR's from different organisms reveals that among only 18 conserved residues, of which most (in B2) either coordinate the iron center or provide the hydrophobic pocket surrounding the

tyrosyl radical, is an additional conserved tyrosine (46). This residue, Y356 in B2, lies in the putative B1-binding domain of the subunit. Whether this conserved tyrosine gives rise to the transient radical observed in B2-Y122F and whether it might play a role in the catalytic mechanism of RNR's remain to be determined.

REFERENCES AND NOTES

1. J. Stubbe, *Adv. Enzymol.* **63**, 349 (1989).
2. L. Thelander and P. Reichard, *Annu. Rev. Biochem.* **48**, 133 (1979).
3. S. Eriksson and B. M. Sjöberg, in *Allosteric Enzymes*, G. Hervé, Ed. (CRC Press, Boca Raton, FL, 1989), pp. 189–215.
4. P. Nordlund, B. M. Sjöberg, H. Eklund, *Nature* **345**, 593 (1990).
5. P. Reichard and A. Ehrenberg, *Science* **221**, 514 (1983).
6. C. L. Atkin, L. Thelander, P. Reichard, G. Lang, *J. Biol. Chem.* **248**, 7464 (1973).
7. B. M. Sjöberg, P. Reichard, A. Gräslund, A. Ehrenberg, *ibid.* **252**, 536 (1977).
8. B. M. Sjöberg, T. M. Locher, J. Sanders-Loehr, *Biochemistry* **21**, 96 (1982).
9. L. Petersson *et al.*, *J. Biol. Chem.* **255**, 6706 (1980).
10. M. Sahlin *et al.*, *Biochemistry* **28**, 2618 (1989).
11. R. C. Scarrow *et al.*, *J. Am. Chem. Soc.* **109**, 7857 (1987).
12. G. Bunker *et al.*, *Biochemistry* **26**, 4708 (1987).
13. J. M. McCormick *et al.*, *New J. Chem.*, in press.
14. J. B. Lynch, C. Juarez-Garcia, E. Münck, L. Que, *J. Biol. Chem.* **264**, 8091 (1989).
15. M. Sahlin *et al.*, *Biochemistry* **26**, 5541 (1987).
16. J. B. Vincent, G. L. Olivier-Lilley, B. A. Averill, *Chem. Rev.* **90**, 1447 (1990); L. Que, Jr., and A. E. Truc, *Prog. Inorg. Chem. Bioinorg. Chem.* **38**, 97 (1990).
17. J. Sanders-Loehr, *Oxidases and Related Redox Systems*, H. S. Mason, T. E. King, M. Morrison, Eds. (Liss, New York, 1988), pp. 193–209.
18. B. G. Fox, K. K. Surerus, E. Münck, J. P. Lipscomb, *J. Biol. Chem.* **263**, 10553 (1988); J. Green and H. Dalton, *ibid.* **264**, 17698 (1989).
19. S. P. Salowe and J. Stubbe, *J. Bacteriol.* **165**, 363 (1986).
20. Extensive (unpublished) EPR experiments to determine the $\text{Fe}^{2+}/\text{Y122}$ stoichiometry have revealed that the ratio observed is somewhat dependent on the method of addition of Fe^{2+} to apoB2. The ratios reported here are those observed under optimum conditions, in which apoB2 in air-saturated buffer is rapidly mixed with limiting Fe^{2+} (1 to 2.2 molar equivalents) or with limiting Fe^{2+} and ascorbate. Experimental details of the determinations are available upon request.
21. E.-I. Ochiai, G. J. Mann, A. Gräslund, L. Thelander, *J. Biol. Chem.* **265**, 15758 (1990). While our work was in progress, Ochiai *et al.* reported the reconstitution stoichiometry for the small subunit (M2) of mammalian RNR. The results reported are quite similar to the values which we find using B2.
22. A. Ehrenberg and P. Reichard, *J. Biol. Chem.* **247**, 3485 (1972).
23. B2 as isolated contains $3.2 \pm 0.3 \text{ Fe}^{3+}/\text{B2}$ and $1.2 \pm 0.1 \cdot\text{Y122}/\text{B2}$, and has a specific activity of $8500 \pm 500 \text{ U/mg}$. Theoretically, the dimeric subunit could contain 4 $\text{Fe}^{3+}/\text{B2}$ and 2 $\cdot\text{Y122}/\text{B2}$. The reason for this discrepancy is unknown. When apoB2 is titrated with Fe^{2+} in the absence of ascorbate, the stoichiometry required for complete reconstitution, while somewhat dependent on the method of addition, is about 4 $\text{Fe}^{2+}/\text{B2}$. In the presence of ascorbate, 3.2 $\text{Fe}^{2+}/\text{B2}$ are required. At the end point of each titration the protein contains $1.15 \pm 0.07 \cdot\text{Y122}/\text{B2}$ and has a specific activity of $7000 \pm 1000 \text{ U/mg}$. For determination of the kinetics of the reaction, an $\text{Fe}^{2+}/\text{B2}$ ratio of 5 was chosen so that Fe^{2+} would be slightly in excess.
24. The rate constants reported are averages from several experiments. They were obtained by fitting the first five seconds of the absorbance-versus-time data to the equation for a first-order growth. However, the limiting Fe^{2+} reaction deviates substantially from first-order behavior; spectral changes in the region of the diferric center continue up to $\sim 40 \text{ s}$. All the rate constants reported should be considered estimates.
25. The k_{obs} makes the reaction amenable to study with a Hewlett Packard HP8452A Diode Array spectrometer, which can acquire an 80-nm spectrum every 0.1 s. It was anticipated that use of this multiple-wavelength detector would facilitate observation of intermediates with unknown spectral features. Therefore, unless otherwise noted, all stopped-flow experiments described were carried out with an Applied Photophysics Rapid Kinetics Spectrometer Accessory in conjunction with the HP8452A spectrometer. Both instruments were triggered manually, resulting in a long and somewhat variable "dead time" [estimated to be 0.1–0.25 s based on comparison of time traces from this apparatus to those obtained on the apparatus described in (27)].
26. The extent of $\cdot\text{Y122}$ production was judged by the dropline corrected absorbance at 412 nm:

$$A_{412, \text{dropline}} = A_{412} - [A_{416} + (A_{406} - A_{416})(416 - 412)/(416 - 406)].$$

Comparison of this quantity in over 80 samples of B2 reconstituted under different conditions to $\cdot\text{Y122}$ determined by EPR spectroscopy has shown $A_{412, \text{dropline}}$ to be an accurate reflection of $\cdot\text{Y122}$.

27. The long, variable dead time of the modified HP apparatus described in (25) required using a Hi-Tech SF-41 Canterbury Stopped-Flow with an SU-40 spectrophotometer to observe the growth and decay of the 565-nm feature. Nonlinear least-squares fitting of the 565-nm absorbance-versus-time curve generated the apparent first-order-rate constants which are reported.
28. The mutant B2-Y122F was prepared using a kit purchased from Amersham. The identity of the mutant was confirmed by DNA sequencing with the chain termination method. The protein was expressed in *E. coli* using a system

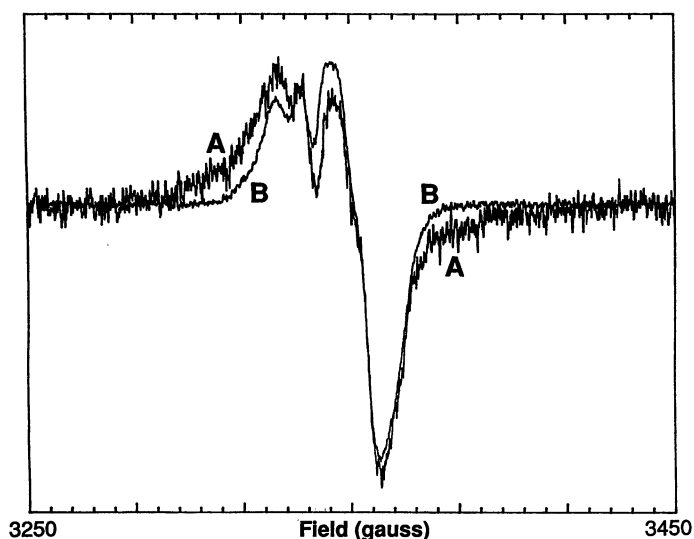


Fig. 9. Broadening of the EPR spectrum of the limiting Fe^{2+} reaction. ApoB2 (100 μM) in air-saturated 100 mM Hepes buffer, pH 7.7 was mixed at 5°C (curve A) with 220 μM or (curve B) with 1.0 mM FeSO_4 dissolved in air-saturated 5 mM HNO_3 . The reactions were quenched at 0.65 s. The spectra were recorded as in Fig. 8.

- developed by Tabor and Richardson [S. Tabor and C. Richardson, *Proc. Natl. Acad. Sci. U.S.A.* **82**, 1074 (1985)]. It should be noted that a small amount (<1%) of chromosomally encoded wild-type B2 is present in preparations of B2-Y122F.
29. Assuming that the molar absorptivity of this unstable tyrosyl radical is the same as that of \cdot Y122, the maximum amount of the transient radical present is $\sim 0.06 \cdot$ Y/B2. The failure of this species to accumulate to a greater extent is most likely a reflection of its instability.
 30. S. Menage *et al.*, *J. Am. Chem. Soc.* **112**, 6423 (1990). Abbreviations used: OBz, benzoate; HPTB, *N,N,N',N'*-tetrakis(2-benzimidazolymethyl)-2-hydroxy-1,3-diamino-propane.
 31. The aforementioned (27) nonlinear least-squares fit to the formation and decay of (U) had an adjustable parameter, the molar absorptivity of the intermediate. ϵ_{565} for (U) was found to be $1500 \text{ M}^{-1} \text{ cm}^{-1}$.
 32. Although there have been several other reports of peroxodiferric model complexes, most of these species have not been characterized as well as the complex of (30). In addition, we believe that the diferrous precursor (I) of (30) more closely approximates the diferrous cluster of B2 than do the precursors to any of the other putative peroxodiferric complexes. Further characterization of (U) is required to establish its structure.
 33. Simulations of the kinetics of the excess Fe^{2+} reaction indicate that (U) must decay with a rate constant greater than 20 s^{-1} (assuming that the rate constant for its formation is 8 s^{-1}) in order to account for the observed failure of the intermediate to accumulate.
 34. D. Dolphin *et al.*, *Proc. Natl. Acad. Sci. U.S.A.* **68**, 614 (1971).
 35. J. E. Erman, L. B. Vitello, J. M. Mauro, J. Kraut, *Biochemistry* **28**, 7992 (1989), and references cited therein.
 36. D. P. Ballou and G. Palmer, *Anal. Chem.* **46**, 1248 (1974).
 37. Pathway A predicts that equal amounts of \cdot Y122 and (X) should be present at short times in the limiting Fe^{2+} reaction. While the spectra of Fig. 7 indicate that some \cdot Y122 is present, there appears to be more (X) present. This apparent discrepancy is probably due to a partition between pathway A and pathway B under limiting Fe^{2+} conditions.
 38. The amount of radical present at 0.33 s was determined by comparing the double integral of the spectrum of this time point (Fig. 8A) to that of the 60 s time point (Fig. 8D). The ratio of \cdot Y122 to B2 at completion of the reaction is known from the stoichiometry studies. A control verified that the freeze-quenching procedure does not cause loss of \cdot Y122. Therefore, the sample of Fig. 8D provides a radical concentration standard for the other samples (Fig. 8).
 39. M. Fontecave, C. Gerez, M. Atta, A. Jéunet, *Biochem. Biophys. Res. Commun.* **168**, 659 (1990).
 40. M. Sahlin *et al.*, *ibid.* **167**, 813 (1990).
 41. D. H. Chin, G. N. LaMar, A. L. Balch, *J. Am. Chem. Soc.* **102**, 4344 (1980).
 42. T. J. McMurtry and J. T. Groves, in *Cytochrome P-450: Structure, Mechanism, and Biochemistry*, P. R. Ortiz de Montellano, Ed. (Plenum, New York, 1986), pp. 1–28.
 43. J. M. Bollinger, Jr., J. Stubbe, D. Edmondson, B. H. Huynh, *J. Am. Chem. Soc.*, in press.
 44. J. Stubbe, M. Ator, T. Krenitsky, *J. Biol. Chem.* **258**, 1625 (1983).
 45. J. Stubbe, *J. Biol. Chem.* **265**, 5329 (1990).
 46. B. M. Sjöberg *et al.*, *FEBS Lett.* **183**, 99 (1985).
 47. Dedicated to R. H. Abeles on the occasion of his 65th birthday. Supported by NIH grants GM29595 (J.S.), GM32187 (B.H.H.), GM29433 (D.E.E.), NSF grants DMB-9001530 (B.H.H.) and CHE-8819760 (J.R.N.), a Whitaker Health Science Fellowship (J.M.B.) and a Guggenheim fellowship (J.R.N. during his stay at Massachusetts Institute of Technology).

11 March 1991; accepted 22 May 1991